Proton Irradiation Effects on Spin Orbit-Torque and Spin- Transfer Torque Magnetic Tunnel Junctions

Odilia Coi, *IEEE Student member* *†‡, Gregory Di Pendina*, Kevin Garello*, David Dangla ‡, Robert Ecoffet ‡ and Lionel Torres †
*Univ. Grenoble Alpes, CNRS, CEA, Spintec, 38000 Grenoble, France
†LIRMM-University of Montpellier, CNRS, France
‡Centre Nationale d'Etudes Spatial (CNES) 31401 Toulouse, France

***Abstract*—This paper aims to investigate proton irradiation effects on a new class of emerging devices: Perpendicular-Magnetic Anysotropy (PMA) Spin Orbit (SOT) Torque Magnetic Tunnel Junctions (MTJ).**

I. Introduction

The recent successful landing of the Mars Perseverance Rover with on board the high performance, space qualified, 16 Mb toggle-MRAM (UT8MR2M8) based on proven technology from Everspin and CAES, demonstrates that Non-Volatile (NV) Magnetic Random Access memory (MRAM) is a key element for future space missions. Certainly, the mission will provide very interesting data on the memory's radiation hardness, however, the main drawbacks of toggle MRAM remain: huge size, writing complexity and poor scalability are unlikely to make it a suitable candidate for future applications [1]. For this reason, looking ahead, a good alternative seems to be the spintronic-based memories, particularly attractive on the market due to their high scalability, good performance, high endurance and low power consumption.

The most common device from this family is the Spin-Tranfer Torque (STT) Magnetic Tunnel Junction (MTJ) a nanometric multi-layer pillar. For the sake of simplicity, it is possible to grouping these layers by recognizing: two ferromagnetic layers with perpendicular magnetic anisotropy (PMA) and a thin oxide tunnel barrier, typically MgO. By construction, one of the two layers has a free switchable orientation (FL) while the other, consisting of pinned oriented spin, is used as reference layer (RL). This way, by allowing a current to flow through the pillar, it is possible to switch the orientation of the FL so that it becomes parallel or antiparallel with respect to the RF, allowing the storage of bit "0" or "1". Indeed, due to the ferromagnetic properties of the CoFeB layer the MTJ cell exhibits low/high resistance depending on the mutual magnetic orientation of these two layers. By means of a current, usually equal to one-third of the writing current, it is possible to sense the state of the device by leveraging on the tunnel magneto-resistance effect (TMR).

The main drawback of STT-MRAM is the shared read/write path which can impair the read reliability. Indeed, the write current can impose a severe stress for the memory cell leading to a possible time dependent degradation of the MTJ. Trying to go beyond this limit, a new proof of concept was presented in [2] and [3] hereby providing a new approach for controlling magnetic device: Spin Orbit Torque Magnetic Tunnel Junction. The latter is a three terminal device where reading and writing paths are decoupled thereby enhancing the robustness of the simple STT-MTJ pillar. Indeed, it no longer needs to be traversed by a large write current, which, instead, passes through a strip of metal underneath, called the SOT channel. This separation significantly enhances the reliability of the device [4] since the write current does not flow through the tunnel barrier, which is sensitive to electrical breakdown. For this motivation SOT devices gained the attention of industry [5] and academia [6] confirming attractive qualities such as a very fast switching, a quasi-infinite endurance and the elimination of the read disturbance. A very attractive design for high density application was recently proposed in [7], where the SOT channel is shared among different device. In [8] they propose radiation hardening by design techniques to enhance the robustness of the complementary metal oxide semiconductor (CMOS) peripheral circuitry needed to write and read the SOT devices.
To the best of our knowledge there is only one study on the irradiation of PMA-MTJ SOT devices and none on the protons irradiation effects, which is the focus of this study. Indeed in [9] it was observed that gamma ionizing dose up to 1 Mrad(Si) does not alter the magnetic switching behavior, while very high Ta^{1+} ion irradiation (over 10^{12} p/cm^2) modified some magnetic properties.

II. Device under test

SOT-MTJ is a three terminal geometry devices where a traditional PMA-STT MTJ is placed on top of a heavy metal strip made of an hard metal such as Pt, W or Ta. Two physical phenomena are understood to be at the origin of the spin-orbit torques: a bulk component, the Spin Hall Effect, and an interfacial component, commonly known as the Rashba Effect. The Spin Hall effect induces a spin current transverse to the charge current flowing in the SOT strip layer, leading to a spin accumulation at the SOT interfaces, which then diffuses into magnetic materials.

The Rashba effect originates from the uncompensated electric field at the interface, resulting in an effective magnetic field directly acting on nearby magnetizations. Both effects lead to magnetic torques, that can control the magnetization

TABLE I
MAGNETO-ELECTRICAL PARAMETERS OF THE DIFFERENT INVESTIGATED SAMPLES

Parameter	Symbol	SOT Value range	STT Value range
Critical Diameter [nm]	$\mathcal{CD}$	60-200	60-1000
Tunnel Magnetoresistance [%]	$\mathcal{TMR}$	10-90	15-140
Barrier Thickness [nm]	$\mathcal{T}_{ox}$	0.8-1	1.1-1.3
Channel lengh [nm]	$\mathcal{T}_c$	4	-
Channel high [nm]	$\mathcal{W}_c$	50	-
Channel high [nm]	$\mathcal{L}_c$	180	-
Channel resistivity [Ω cm]	ρ	20	-

direction of an adjacent magnetic free layer. This way, it is possible to write a binary "0" or "1" in the MRAM cell. Indeed, SOT-MRAM devices feature switching of the free magnetic layer done by injecting an in-plane current in the SOT channel. Unlike STT-MRAM, where the current is injected perpendicularly into the magnetic tunnel junction and the read and write operation is performed through the same path, the Spin Orbit Torque effect converts charge into spin current, which enables also ultra-fast switching (see Fig. 1). The read principle is the same as for the STT: a charge-flow through the MTJ is employed to sense the magnetization state of the device through the magneto-resistance phenomena, i.e. the change in the material conductivity depending on the mutual magnetization state of the reference and free layer. SOT uses the same core MTJ as the existing STT and can thus be easily implemented in the same manufacturing environment as STT. In this study, we irradiated both SOT and STT devices

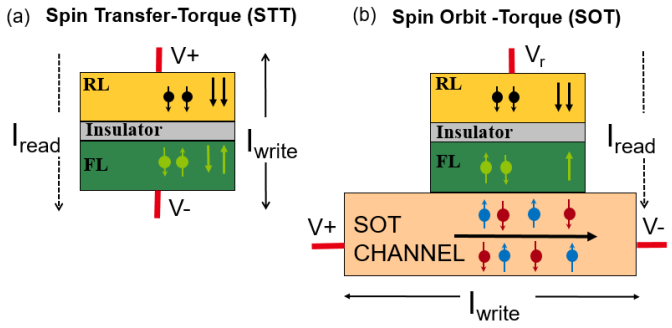

Fig. 1. Schematic view of STT and SOT reading/writing paths

so that we can make a comparison on the irradiation response of these two technologies. The devices were organized in 2 groups: first group was irradiated with 62 MeV protons to a fluence of 1.2 x 10 ^{11} p/cm^2 (F1), while a fluence of 1.2 x 10^{12} p/cm^2 (F2) was chosen for the second group. The flux was set to the maximum value the facility could provide: 2 x 10^8 p/cm^2/s. Each group of SOT and STT consisted of 25 magnetic elementary memory arrays arranged in 6 column x 9 rows. Each row hosted different MTJ sizes as highlighted in Table I. They were fabricated by a SPINTEC partner to guarantee an industrial process using the most advanced CoFeB-MgO technology. As depicted Fig. 2 samples have a cross bridge structure of two metal wires for the top and bottom electrodes,

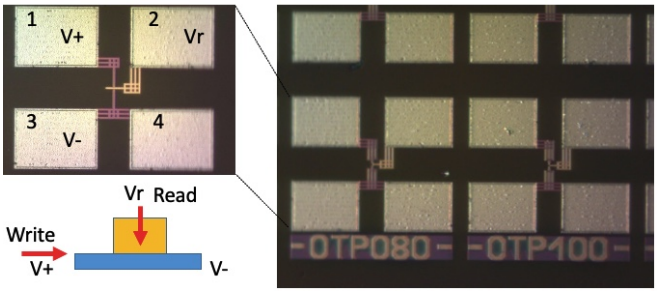

Fig. 2. Photomicrograph of the purely magnetic SOT memory. The 4 pads and the MTJ device are highlighted as well as the correspondence with the device cartoon

which have been used to make three-terminal measurements. Indeed, prior to irradiation a set of measurements were done:

- The resistance and TMR
- The coercive field H_c, i.e. the field value needed to switch the magnetization from one stable state to the other, which in a perfectly symmetrical situation, corresponds to one half of the whole hysteresis loop width. Its value is considered as positive for the P to AP transition, and negative conversely.
- The offset field H_{off}, which quantifies the hysteresis loop shift with respect to a symmetrical situation.

Each measurement is the result of a 300 times cycle performance, which were made in partnership with Hprobe, a company leader in characterization and testing of MRAM. All the MTJs were set in the parallel state (R_{min}) because in these devices, by construction, the favored (i.e. more stable) configuration is the antiparallel (R_{max}). This is due to choices made at the level of the multi-layer stack to compensate dipolar fields across the device.

III. EXPERIMENTAL RESULT

The experimental radiation campaign was performed at the UCL Cyclotron (Université Catholique de Louvain), of Louvain-la-Neuve. Each MTJ receives at least 3 protons hits. This is a worst case scenario, calculated for the smallest magnetic structure at the lowest fluence.

After-irradiation measurements show that devices exposed to the lowest proton fluence do not experienced any relevant change in their parameters.

In respect of the devices exposed to F2, due to the large amount of analyzed data we decided to plot, for the sake of clarity, the median value and the standard deviation of each parameters, for each size, before and after irradiation. In case of detected anomalies we then go further and show also the typical Inter quartile Range (IQR) analysis, namely the box plot.

A. Electrical properties

The study shows how median value and standard deviation of resistance are immune to protons irradiation for both STT (Fig. 4 a) and SOT (Fig. 5 a) MTJs. Consequentely no Single Event Upset occureed due to the irradiation.

As Fig. 4 b depicts, the median value of TMR after irradiation decrease up to 11% depending of the STT sizes. This is not the case with SOT: the TMR remains stable before and after irradiation, as clearly represented in Fig. 5 b. However, taking into account human-factor in the positioning of the test machine probe and the machine sensitivity, this variation could be within the estimated error tolerance range for this experiment. Anyway, the ability to correctly read the memory state whith such TMR values is still is preserved.

B. Magnetic properties

The median value of the coercive field after irradiation is somewhat larger than before both for STT (10%-17%) (Fig. 4 c) and SOT (10%-20%) (Fig. 5 c) devices.

However, to gain more insights, these data should be analyzed together with the H_{off} ones. Concerning the STT-MTJs, the changes in H_{off} distribution are quite evident (Fig. 4 d). By observing the latter figure, it is noticeable, in three-quarters of cases, a change in the median distribution, accompanied with an augmentation of the standard deviation. On the contrary, in the case of SOT-MTJs, H_{off} does not experience a change as relevant as in the STT-MTJ case, as plotted in Fig. 5 d. In order to bring more understanding, the IQR distribution of H_{off} for STT devices is reported in Fig. 6. The box plots after irradiation appear stretched. In particualar, in two-third of cases the distribution of the first and second quartile is very broad leading to a left-skewed distribution. For the sizes equal to 100 nm, 120 nm and 150 nm this represents a change with respect to the right-skewed pre-irradation distribution.

By remembering the mathematical meaning of H_{off} as:

$$H_{\text{off}} = \frac{H_c - |-H_c|}{2} \tag{1}$$

we can easily understand the implication of the experimental observation: statistically, the absolute value of H_c has increased, i.e the transition from AP to P to state after irradiation takes place at a more negative value. This is reflected in the shape of the hysteresis loop which loses its symmetry: the majority of the hysteresis loop shifted towards the left for STT devices. Fig. 3 shows the hysteresis loop in the two cases: $H_{off} < 0$ (a) and $H_{off} > 0$ (b).

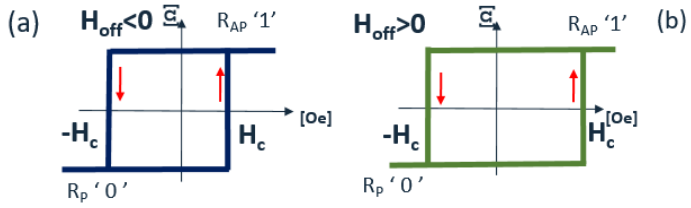

Fig. 3. Hysteresis loop shape in case of $H_{off} < 0$ (a) and $H_{off} > 0$ (b).

IV. Conclusion

A comparative study on SOT and STT elementary structures demonstrates electrical properties to be unaffected up to the highest proton fluence used in this campaign, i.e. 1.2 x 10^{12} p/cm^2. Simultaneously, a slight increase of the positive coercive field is observed for both the categories of devices. Offset field variations are noticeable for STT devices, to the point that the parameter changes its sign. A closer look at the H_{off} box plot distribution made it possible to conclude that the negative coercive field (transition from AP to P) has increased in absolute value. On the contrary, H_{off} parameter does not experience significant changes in the SOT samples.

Diverse hypothesis could explain these experimental findings. As first, the fact that the writing current in SOT devices does not flow into the MTJ, thence structural changes in the MgO barrier or other layers will affect less the writing process. As second, the difference in the MTJ nano-pillar materials between SOT and STT and, as third, the order of these multilayers. Indeed, in SOT device the free layer has to be on top of the heavy metal strip, while for STT it could be positioned on the top or bottom with respect to the reference layer.

In conclusion, this study suggests SOT devices as better candidate than STT ones for future space applications. Nevertheless further experiments are needed to clarify the motivations which lead to this consequence.

References

[1] B. Dieny, R. Goldfarb, and K.-J. Lee, *Introduction to Magnetic Random-Access Memory*, Hoboken, Wiley-IEEE Press, USA, Nov. 2016.

[2] K. Garello, I. M. Miron, G. Gaudin, P. J. Zermatten, M. Costache, S. Auffret, S. Bandera, B. Rodmacq, A. Schuhl, and P. Gambardella, "Perpendicular switching of a single ferromagnetic layer induced by in-plane current injection," in *APS March Meeting Abstracts*, ser. APS Meeting Abstracts, vol. 2012, Feb. 2012, p. P15.010.

[3] L. Liu, C.-F. Pai, Y. Li, H.-W. Tseng, D. Ralph, and R. Buhrman, "Spin-torque switching with the giant spin hall effect of tantalum," *Science (New York, N.Y.)*, vol. 336, pp. 555–8, 05 2012.

[4] P. Gambardella and I. M. Miron, "Current-induced Spin–orbit torques," *Philosophical Transactions of the Royal Society A: Mathematical, Physical and Engineering Sciences*, vol. 369, pp. 3175 – 3197, 2011.

[5] K. Garello, F. Yasin, and G. S. Kar, "Spin-orbit torque mram for ultra-fast embedded memories: from fundamentals to large scale technology integration," in *2019 IEEE 11th International Memory Workshop (IMW)*, 2019, pp. 1–4.

[6] G. Prenat, K. Jabeur, P. Vanhauwaert, G. D. Pendina, F. Oboril, R. Bishnoi, M. Ebrahimi, N. Lamard, O. Boulle, K. Garello, J. Langer, B. Ocker, M.-C. Cyrille, P. Gambardella, M. Tahoori, and G. Gaudin, "Ultra-fast and high-reliability sot-mram: From cache replacement to normally-off computing," *IEEE Transactions on Multi-Scale Computing Systems*, vol. 2, no. 1, pp. 49–60, 2016.

[7] R. Mishra, T. Kim, J. Park, and H. Yang, "Shared-write-channel-based device for high-density spin-orbit-torque magnetic random-access memory," *Phys. Rev. Applied*, vol. 15, p. 024063, Feb 2021. [Online]. Available: https://link.aps.org/doi/10.1103/PhysRevApplied.15.024063

[8] B. Wang, Z. Wang, B. Wu, Y. Bai, K. Cao, Y. Zhao, Y. Zhang, and W. Zhao, "Novel radiation hardening read/write circuits using feedback connections for spin–orbit torque magnetic random access memory," *IEEE Transactions on Circuits and Systems I: Regular Papers*, vol. 66, no. 5, pp. 1853–1862, 2019.

[9] M. Alamdar, L. J. Chang, K. Jarvis, P. Kotula, C. Cui, R. Gearba-Dolocan, Y. Liu, E. Antunano, J. E. Manuel, G. Vizkelethy, L. Xue, R. Jacobs-Gedrim, C. H. Bennett, T. P. Xiao, D. Hughart, E. Bielejec, M. J. Marinella, and J. A. C. Incorvia, "Irradiation effects on perpendicular anisotropy spin–orbit torque magnetic tunnel junctions," *IEEE Transactions on Nuclear Science*, vol. 68, no. 5, pp. 665–670, 2021.

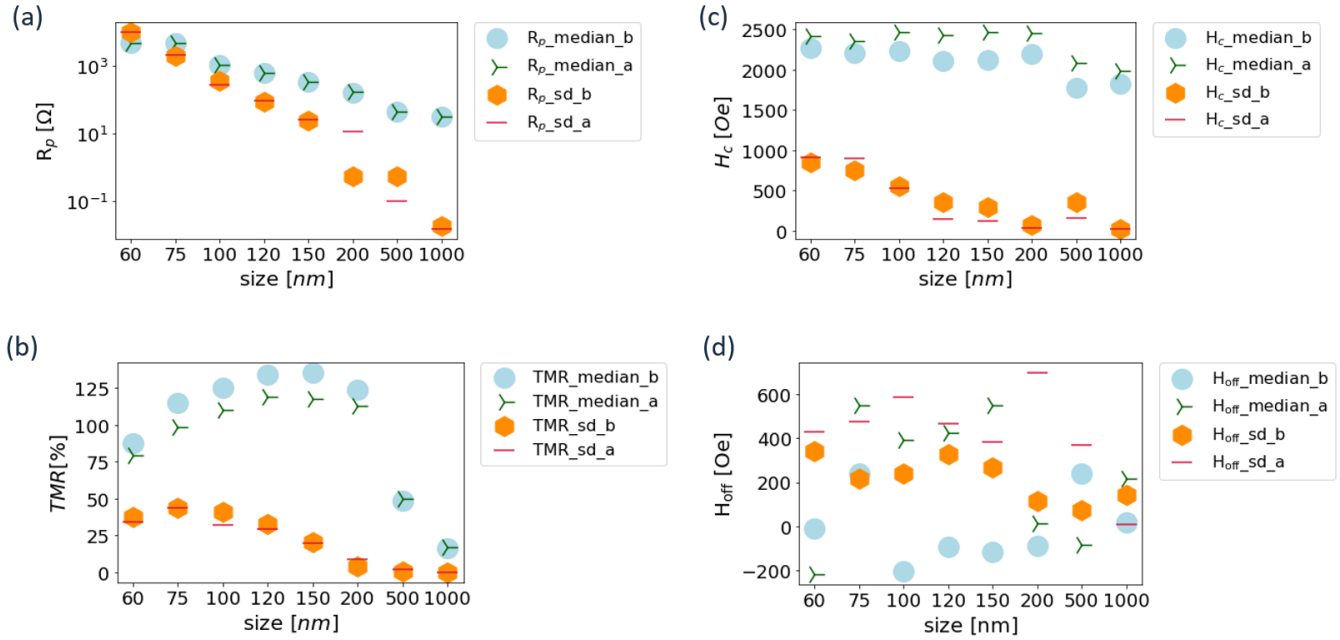

Fig. 4. Median and standard deviation before and after the F2 irradiation for the STT-MTJs parameters: Resistance (a),TMR (b), H_c (c), H_{off} (d)

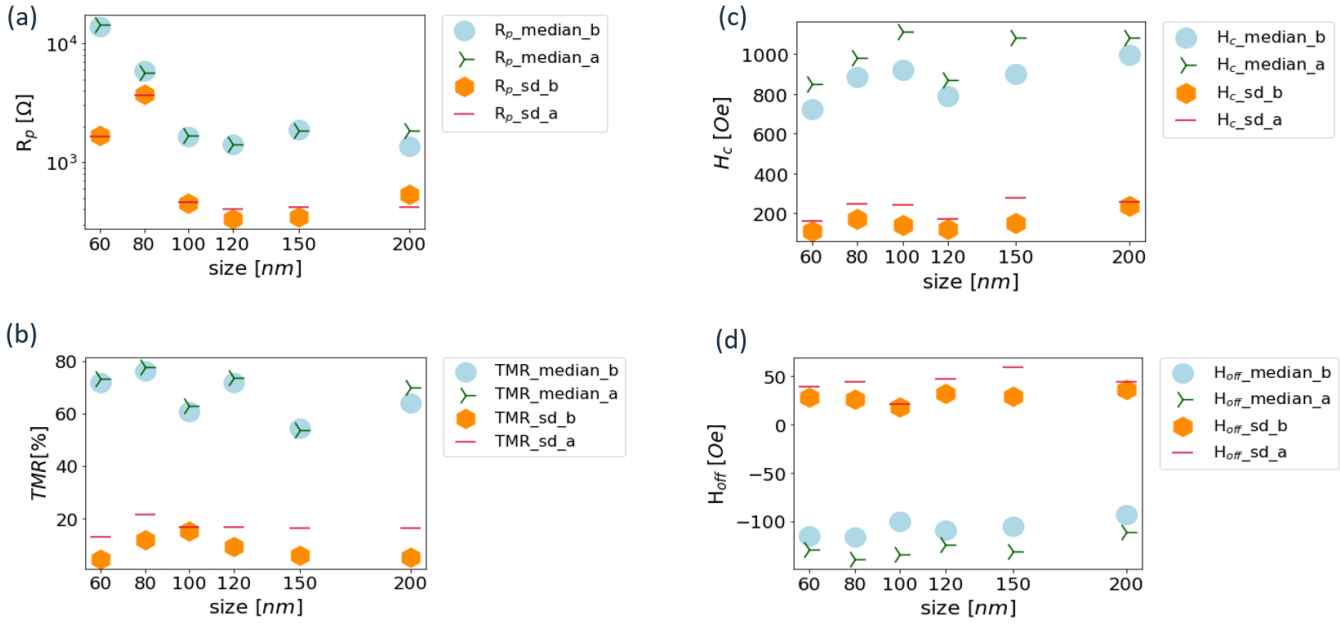

Fig. 5. Median and standard deviation before and after the F2 irradiation for the SOT-MTJs parameters: Resistance (a),TMR (b), H_c (c), H_{off} (d)

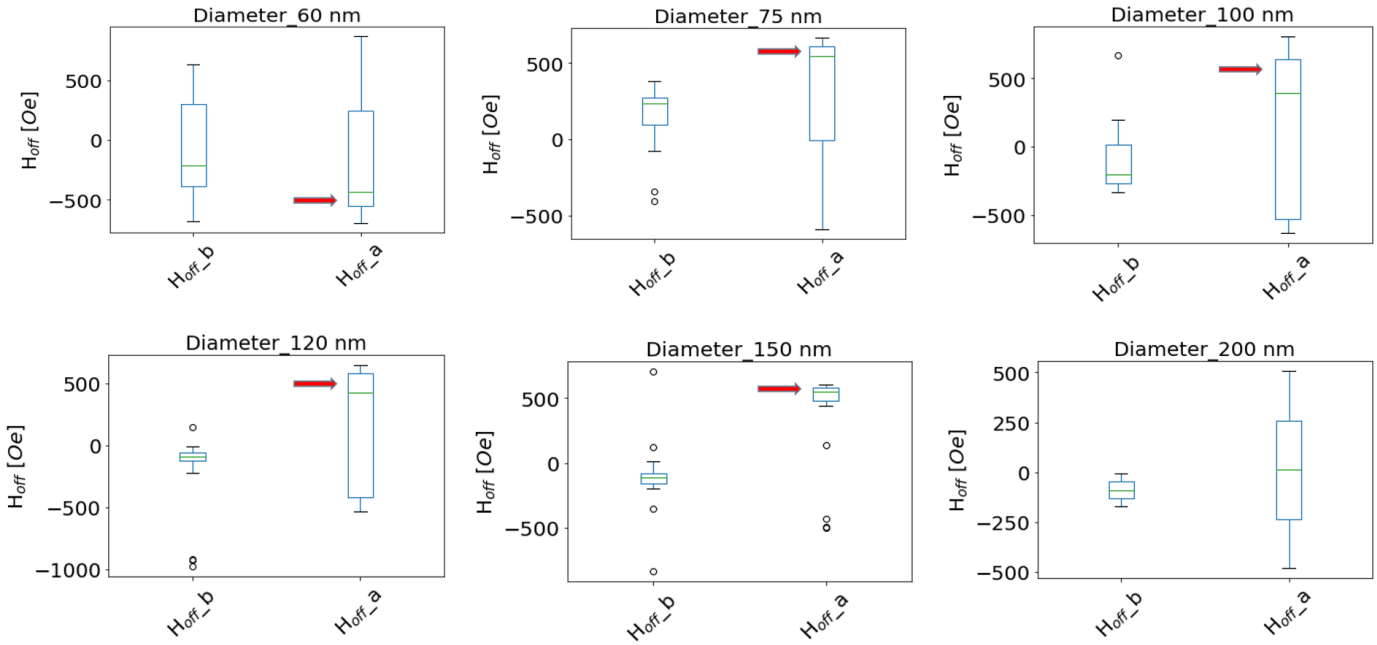

Fig. 6. H_{off} IQR distribution before and after F2 irradiation for different STT sizes. The red arrows highlight how broader the first and second quartile distributions became.